Hindawi
Shock and Vibration
Volume 2019, Article ID 7080941, 12 pages
https://doi.org/10.1155/2019/7080941

Research Article

The Spherical Shock Factor Theory of a FSP with an Underwater Added Structure

Guo Jun,[1] **Yong Yang**,[1] **Yin Zhang**,[1] **and Lin-han Feng**[2]

[1]*College of Shipbuilding Engineering, Harbin Engineering University, Harbin 150001, China*
[2]*Naval Research Academy, Beijing 100000, China*

Correspondence should be addressed to Guo Jun; guo_jun@hrbeu.edu.cn

Received 11 September 2018; Revised 6 November 2018; Accepted 17 December 2018; Published 13 January 2019

Academic Editor: Chengzhi Shi

A floating shock platform (FSP) is important experimental equipment for the antishock assessment of large-scale shipborne equipment. Generally speaking, the FSP is a square barge structure with a flat bottom. In order to satisfy the key index of the horizontal-to-vertical ratio of the impact environment, a special added structure is mounted to the bottom of the platform, and the impact environment is more complicated due to the added structure. Therefore, the spherical shock factor theory is proposed to analyze the impact environment, and the validity of the theory is proved by numerical experiments. The results show that the average impact spectrum response of the platform is essentially consistent under the same shock factor. Meanwhile, the spherical shock factor builds a linear relationship between the input parameters and structural response, which is convenient for the prediction of impact response.

1. Introduction

The antishock ability of shipborne equipment on a warship is directly related to a warship's combat effectiveness and survivability. In order to reduce the possibility of shipborne equipment being damaged after it is subjected to an explosion, countries all over the world attach great importance to the impact resistance ability of shipborne equipment, and corresponding experimental methods have been developed. In terms of standard formulations, German standard BV043/85 [1] stipulates the equipment impact resistance standard from the point of the installation site, and US military standard MIL-S-901D [2] stipulates in detail the equipment impact resistance standard with 8 aspects that include weight, impact level, and category. At the same time, a special experimental device for shipborne equipment impact resistance has been designed by the US Navy. Fluid-structure coupling subject to an underwater explosion is a very complex problem. Therefore, in the study of fluid-structure coupling theory, the transient fluid-structure interaction mechanisms of a three-dimensional spherical shell and a ship's stiffened plate were studied when subjected to an underwater explosion [3]. Through numerical simulation and experimentation, the fluid characteristics and fluid-structure coupling interactions of damaged ships in the process of submergence are analyzed [4]. Considering the complex input-output relationship of structure impact resistance subject to an underwater explosion, the KSF [5] (keel shock factor) is used to describe the severity of impact. The impact environment of a cylindrical shell subject to an underwater impact was compared and analyzed with different shock factors. It shows that, as a similarity parameter, the new shock factor can effectively reflect the response of an underwater explosion load, and the shock factor also has a certain feasibility for being used to describe the impact environment of a submarine [6]. The improved shock factor indicates that cylindrical and spherical shells have the same impact response [7]. Literature [8] uses the new shock factor to certify the impact environment similarity of a SWATH (small waterplane area twin hull) subject to an underwater explosion. When it comes to impact environment prediction, one author [9] uses the shock factor to predict the impact environment but does not take the difference of the hull and the equipment into account in the installation, and

the shock factor has greater limitations itself. According to the type of ship and device, the position and the angle of incidence of the charge, and other factors, one researcher [10] summarizes the empirical formula of the impact environment, but the accuracy of the formula is not strictly checked, and the scope of application is not strictly defined.

In this paper, to satisfy the key index of the impact environment (shock spectrum [11, 12]) that the horizontal-to-vertical ratio of equipment antishock examination in UNDEX, the added structure is added to the bottom of the FSP, while the impact environment of the added structure is not considered. Since the added structure makes the impact environment of the FSP more complicated, the spherical shock factor theory is used to analyze the complex input-output relationship of the IFSP (irregular floating shock platform) impact environment, and the shock factor is used to predict the impact environment of the IFSP, which will guide the design, manufacture, and installation of the equipment.

2. The Spherical Shock Factor Theory of the IFSP

When the structure is subject to UNDEX, for the sake of reflecting the impact environment characteristics, different regularities of shock spectrum change with the parameters such as conditions, geometric conditions, medium, and etcetera. One researcher [6] thoroughly illustrates the shock factors C_1 and C_2. The keel shock factor C_1 is difficult to use to correctly reflect the underwater explosion impact environment of the cylinder. C_2 is based on the plane wave hypothesis and defined from the angle of energy shielded by the structure, which reflects the similarity of underwater explosion loads in the far field. However, the plane wave assumption cannot be held in the near field. Therefore, in this paper, a new shock factor C_3 is considered to describe the shock energy absorbed by platform, namely, the impact strength received by platform.

2.1. Basic Model and Theoretical Analysis of the Shock Factor. In an explosives experiment, charge weight, explosive distance, and structural characteristics are closely related to the impact environment. In order to study the similarity parameter which reflects the impact environment of the underwater explosion, one can assume that the shock wave is a spherical wave, so the energy born in an explosion can be expressed as follows [13]:

$$E = W\rho_e\eta_e, \tag{1}$$

where ρ_e is the chemical energy per unit mass of charge, η_e is the conversion of chemical energy to shock wave energy, and W is the charge weight (kg).

In an infinite fluid field, the shock wave energy is considered to be distributed over the entire spherical shock wave surface. Thus, the spherical shock wave energy absorbed by the structure is given by

$$E_s = E\frac{S_e}{4\pi R^2} = \frac{\rho_e\eta_e}{4\pi}\frac{WS_e}{R^2} = \frac{\rho_e\eta_e}{4\pi}C_3^2, \tag{2}$$

where E_s is the shock wave energy absorbed by structure, S_e is the projection area of the structure on the wave surface, and R is the shortest distance from the charge to the hull.

The shock factor C_3 is defined as follows:

$$C_3 = \sqrt{S_e}\cdot\frac{\sqrt{w}}{R} = \sqrt{w}\cdot\frac{\sqrt{S_e}}{R} = \sqrt{W\Omega}, \tag{3}$$

where S_e is the area truncated by the solid angle and Ω [14] is the solid angle.

It can be seen from formula (2) that E_s is in proportion to C_3^2, and the shock factor is the unique variable in the expression. C_3 includes the information of the charge weight, the detonation distance, and the structural geometry characteristics of the platform. Therefore, if C_3 is equal under different conditions when the charge is relative to different positions of the structure, the average shock spectrum response of the structure should be essentially consistent and C_3 should fully reflect the characteristics of the impact environment. According to formula (3), the calculation method of Ω under a spherical wave is explained as follows, using a simple rectangular plate.

Figure 1 shows the physical model and geometric relationship of a simple rectangular plate under a spherical shock wave. The vertex Z_0 of the angle Ω is located on the central axis of the rectangular plate. From the symmetry, we can calculate the angle Ω of the whole rectangle using the quarter of the rectangle in the graph. The length of the rectangle is $2a$, and the width is $2b$. The length of the small rectangle is a, and the width is b. Arbitrarily taking the area microelement dS in the small rectangle, the angle of axis Z and the line between the area microelement and vertex Z_0 is given by

$$\theta = \arccos\frac{Z_0}{\sqrt{x^2 + y^2 + Z_0^2}}. \tag{4}$$

The solid angle of the area microelement to the vertex Z_0 is given by

$$d\Omega = \frac{dS\cdot\cos\theta}{L^2} = \frac{Z_0\,dx\,dy}{\left(x^2 + y^2 + Z_0^2\right)^{3/2}}. \tag{5}$$

The solid angle of the small rectangle to the vertex Z_0 is given by

$$\Omega = \int_0^b\int_0^a \frac{Z_0}{\left(x^2 + y^2 + Z_0^2\right)^{3/2}}\,dx\,dy. \tag{6}$$

The integral of formula (6) needs to be solved by numerical methods. It can be seen from formula (6) that the integral function is known, so the calculation of the solid angle is transformed into the determination of integral range. If the integral range is determined, the solid angle of the structure corresponding to the spherical shock wave can

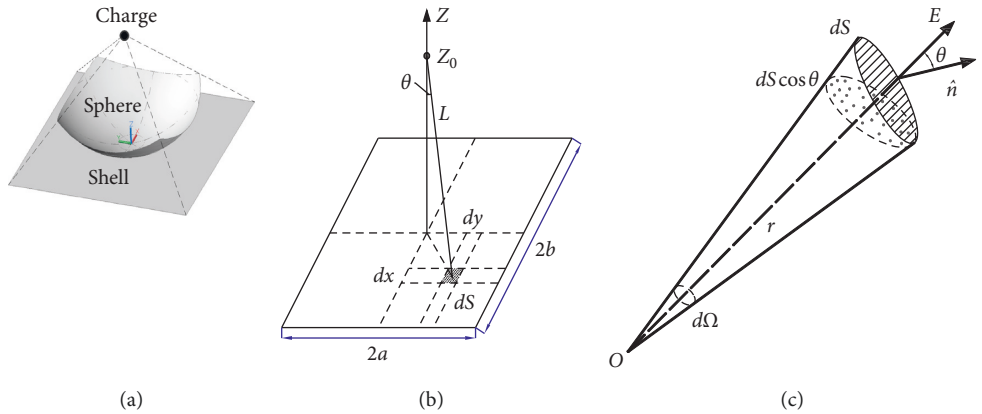

Figure 1: Solid angle calculation diagram of a rectangular plate.

be calculated; consequently, the corresponding shock factor can be obtained.

2.2. Spherical Shock Factor of the IFSP. For the IFSP, the solid angle of the structure on a spherical surface with radius R can be solved similarly to the method used for the rectangular plate. When calculating the shock factor, the charge is located in the transverse section of the platform. Due to the existence of the underwater added structure, the accurate calculation of the solid angle is very complicated, and it needs to be integrated separately along the boundary of the platform. In order to simplify the boundary conditions according to different locations of the charge, the calculation of the shock wave area shielded by the structure is divided into 6 regions as shown in Figure 2.

Taking region S_3 as an example, the local coordinate system xyz is established at the contact point between the platform and the shock wave, and the global coordinate system XYZ is established at the intersection points of the starboard side and the waterline plane, where axes x and X lie along the longitudinal line of the platform. Due to the manufacturing technology, the actual added structure is a little shorter than the platform, but this has no effect on the calculation of the solid angle, so the added structure can be regarded as the same length as the platform. The geometric relationship of the IFSP is shown in Figures 3 and 4, and the fixed geometric parameters in the graph are defined in Table 1.

2.2.1. Starboard Conditions. When the charge is located on the starboard side of the platform, according to the position relationship between the charge and platform, there are three cases:

(a) If $H > T$ and $\varphi < \psi$, there is $\tan(\psi + (\pi/2))$ $L - T > -H$.

From Figure 5, the geometric relation can be given as follows:

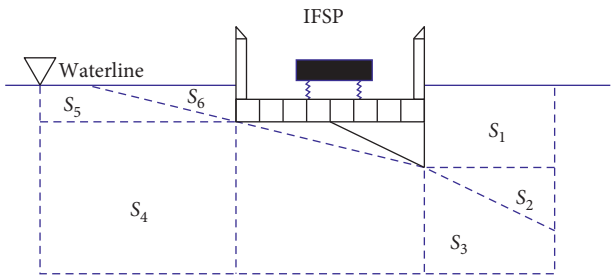

Figure 2: Side view of the IFSP.

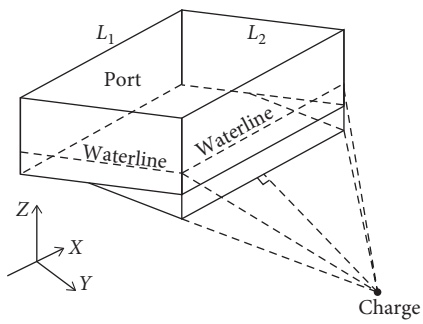

Figure 3: Geometric view.

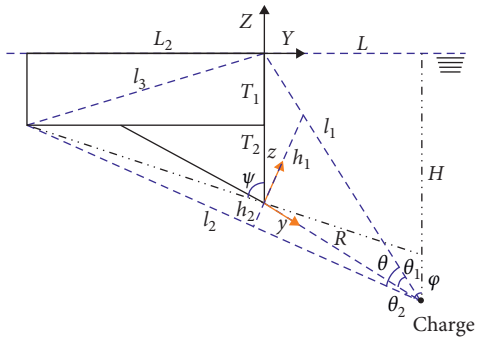

Figure 4: Side view of charge at S_3.

Table 1: Geometric parameters definition.

T_1	Platform draft
T	Structure draft, $T = T_1 + T_2$
l_1	The nearest distance from the charge to the intersection point of the platform and the waterline
T_2	Added structure height
L	The transverse distance from the charge to the structure
H	Depth of charge

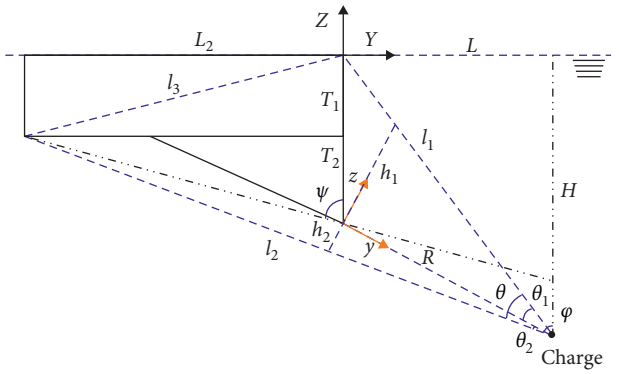

Figure 5: The condition at S_3.

$$\theta = \arccos\frac{l_1^2 + l_2^2 - l_3^2}{2l_1l_2},$$

$$\theta_1 = \arccos\frac{R^2 + l_1^2 - T^2}{2Rl_1},$$

$$\theta_2 = \theta - \theta_1, \tag{7}$$

$$h_1 = R\tan\theta_1,$$

$$h_2 = R\tan\theta_2,$$

$$\Omega = 2\int_{-h_2}^{h_1}\int_0^{L_1/2}\frac{R}{(x^2 + z^2 + R^2)^{3/2}}\,dx\,dz. \tag{8}$$

The integral function of the other cases is the same as formula (8), so it is only necessary to give the integral limits h_1 and h_2.

(b) In Figure 6, if $H > T$ and $(\pi/2) \geq \varphi \geq \psi$, there is $\tan(\psi + (\pi/2))L - T \leq -H$:

$$\theta_1 = \arccos\frac{R^2 + l_1^2 - T^2}{2Rl_1},$$

$$h_1 = R\tan\theta_1, \tag{9}$$

$$h_2 = 0.$$

(c) In Figure 7, if $H \leq T$, there is $h_1 = H$ and $R = L$:

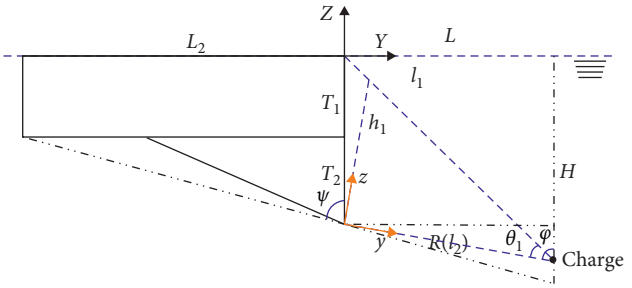

Figure 6: The condition at S_2.

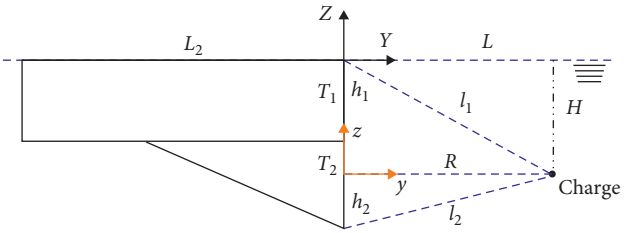

Figure 7: The condition at S_1.

$$h_1 = H,$$
$$h_2 = T - H. \tag{10}$$

2.2.2. Port Conditions. When the charge is located in the port side of the platform, according to the position relationship between the charge and the platform, there are three cases.

(d) In Figure 8, if $H > H_1$, there is

$$\theta = \arccos\frac{l_1^2 + l_2^2 - l_3^2}{2l_1l_2},$$

$$\theta_1 = \arccos\frac{R^2 + l_1^2 - H_1^2}{2Rl_1}, \tag{11}$$

$$\theta_2 = \theta - \theta_1,$$

$$h_1 = R\tan\theta_1,$$

$$h_2 = R\tan\theta_2.$$

(e) In Figure 9, if $H \leq H_1$ and $\varphi_1 < \psi_1$, there is $\tan(\psi + (\pi/2))(-L - L_2) - T > -H$:

$$h_1 = H,$$

$$h_2 = R\frac{T - H}{L + L_2}. \tag{12}$$

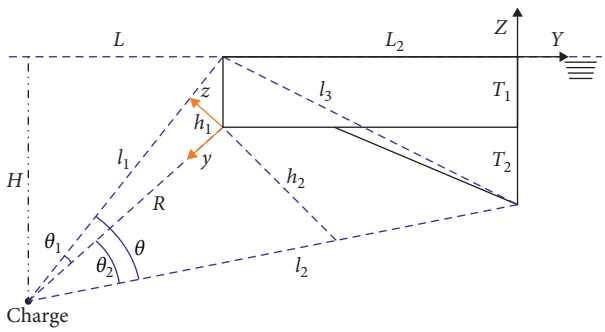

Figure 8: The condition at S_4.

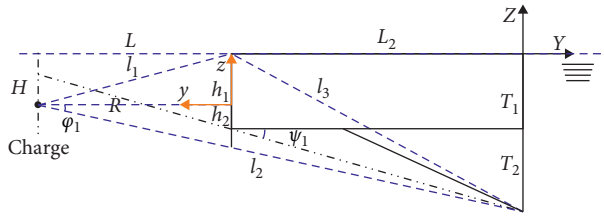

Figure 9: The condition at S_5.

(f) In Figure 10, if $H \le H_1$ and $\varphi_1 \ge \psi_1$, there is $\tan(\psi + (\pi/2))(-L - L_2) - T \le -H$:

$$\begin{aligned} h_1 &= H, \\ h_2 &= H_1 - H. \end{aligned} \tag{13}$$

In all of the above cases, the basic theory is similar to formula (8), so it is only necessary to modify the parameters of various conditions according to the definition.

3. The Numerical Model Establishment and Simulation Analysis of the IFSP

Literature [15–20] shows that numerical methods make it easier for researchers to understand the response characteristics of structures. In order to study the impact of the environmental characteristics of the IFSP subject to an underwater explosion, an underwater explosion numerical model of the platform is established, and the experimental data are used to verify the accuracy of the model. In this paper, the model is prepared for the experimental data that are needed for the prediction of the platform's impact environment.

3.1. The Establishment of Numerical Model. In order to make the numerical model approximate to the real structure and simplify the calculation, the model is established using a three-dimensional finite element model. The numerical simulation algorithm uses the acoustic-structure coupling method, the acoustic medium is used to describe the fluid, and the shock wave propagates in the acoustic element. The platform is in the form of a double bottom structure in the finite element model, the inner bottom and outer bottom are

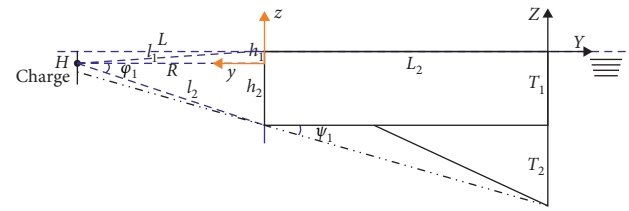

Figure 10: The condition at S_6.

connected by a longitudinal girder and rib, and the surrounding walls are shock resistant bulkheads. Based on the platform width $B = 9$ m, the nondimensional principal dimensions of the model are shown in Table 2; the fluid field is composed of a half cylinder and two quarter spheres.

All mesh sizes of the platform are 5 cm. The girder of the platform and the strengthened beam are composed of first order shear deformation spatial beam elements, and there are about 11,000 elements. The stiffened plate between the girders of the platform and the stiffened beam ,and the outer plates are all composed of quadrilateral or triangular shell elements, which have a linear reduction integral, and there are about 611,000 elements. The fluid field is composed of the linear tetrahedron acoustic medium element, AC3D4. The internal mesh size of the fluid field is 25 cm, external mesh is four times as large as the internal mesh, and there are about 700,000 elements. Finally, a coupling constraint "tie" is added to the underwater interface between the IFSP and fluid field in ABAQUS, which ensures the loads act on platform effectively, and the nonreflecting boundary conditions are established at the external boundary surface of the fluid field. The finite element model of the IFSP subject to an underwater explosion is shown in Figures 11 and 12.

3.2. Model Test on the Basis of the Experiment. As we know, in the course of the model and actual underwater explosion tests, the acceleration response can directly reflect the stress of the local structure which is easy to obtain. In order to describe the underwater explosion impact environment of the FSP, generally, the shock spectrum in a four-dimensional coordinate system is used to analyze the impact. According to structural mechanics, for a single degree-of-freedom system, the relationship between the spectral displacement, spectral velocity, and spectral acceleration of a mass block is given by

$$\begin{aligned} V(\omega) &= \omega D(\omega), \\ A(\omega) &= \omega V(\omega). \end{aligned} \tag{14}$$

It can be seen from formula (14) that the spectral velocity is a link parameter between spectral displacement, spectral acceleration, and vibrator frequency. Therefore, this paper will focus on the spectral velocity in the impact environment.

According to the established numerical model of the IFSP, the charge is located to the side of the added structure in the cross section of the IFSP, and the equivalent quantity of TNT is 150 kg for the charge, with a depth of 6.5 m and a transverse distance of 16 m. The position of detonation point specific conditions of the test and the numerical simulation

Table 2: The principal dimensions of the model.

Model object	Length	Width	High/radius
FSP	2.1B	B	0.8B
Underwater added structure	1.8B	0.6B	0.3B
Fluid field	2.1B	6B	3B

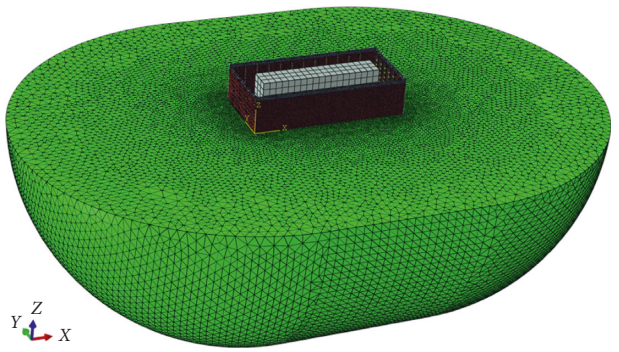

Figure 11: Finite element model subject to underwater explosion.

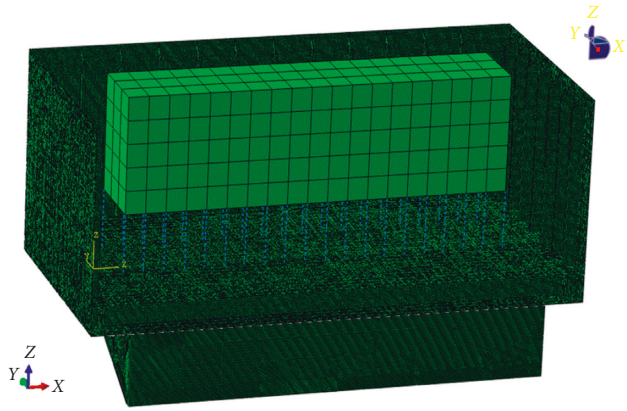

Figure 12: Finite element model of the IFSP.

are shown in Figures 13–15(a), and the platform impact environment test points are shown in Figure 15(b).

The design spectrum in shock spectrum is shown in Figure 16 on the basis of experimental data; it can be seen that the spectral velocity of the simulation is very close to the test at points A, B, and C, and the gap of point D is a little bigger. To estimate the errors between the simulation and test, the comparison of the specific values is shown in Table 3.

The following conclusions are drawn from Table 3: (1) the maximum error of the horizontal spectral velocity is 25.33% between the simulation and the test, the average error of the inner bottom is 7.13%, the maximum error of the vertical spectrum velocity is 26.75%, and the average error of the inner bottom is 19.33%. (2) The error of the vertical and horizontal spectral velocities at the same point is extremely close, and the results show that the simulation results are consistent for the whole model. (3) Except for individual points, the error between the simulation and test is less than 15%, and the error of the impact environment on bottom is

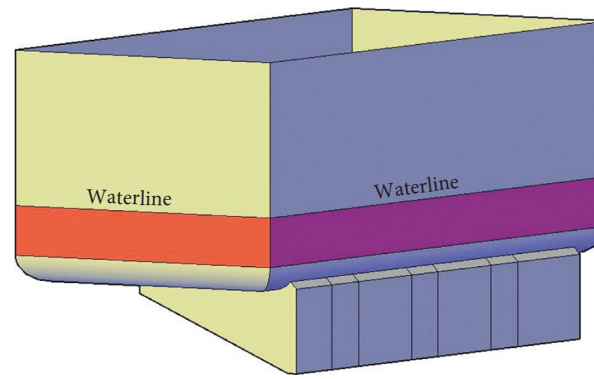

Figure 13: Irregular floating shock platform.

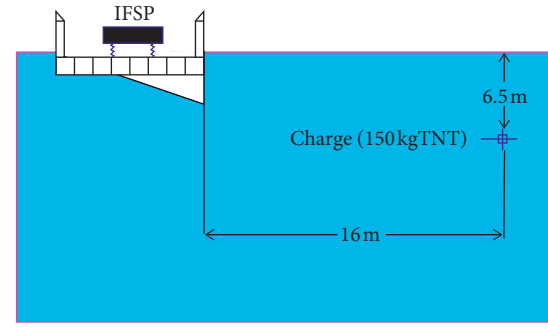

Figure 14: Calculation diagram of the underwater explosion condition.

within 20%. Therefore, the finite element model can effectively simulate the impact environment of the platform.

4. Analysis of the Impact Environment on the Basis of the Spherical Shock Factor

As a similarity parameter of underwater explosion, the problem of the complex input-output relationship of the impact environment on IFSP can be solved by the shock factor. This section is going to examine whether the average impact response spectrum of the IFSP is consistent and use the definition of the shock factor to predict the impact environment.

4.1. Analysis of the Relationship between the Shock Factor and the Impact Environment. Based on the definition of the spherical shock factor, in order to reflect the effect of various parameters to impact environment, the conditions of $C_3 = 6.45$ are shown in Tables 4 and 5 by changing the value of various parameters which include the charge weight, depth, and transverse distance. The established numerical model is used to calculate the average response of the platform under various conditions, and the results shown in Tables 6 and 7 are used to investigate whether the shock factor reflects the average shock spectrum response of the structure.

The comparison of impact response is shown in Figures 17 and 18. It can be seen that when the shock factor is equal, with changes of W, H, and L, the maximum error of the

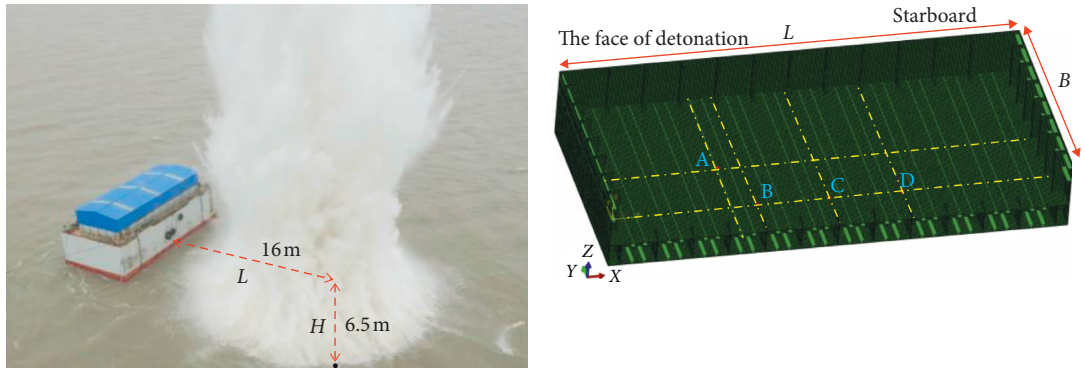

(a) (b)

Figure 15: The explosive experiment of the IFSP. (a) Explosive experiment. (b) Test points of the Platform at the inner bottom.

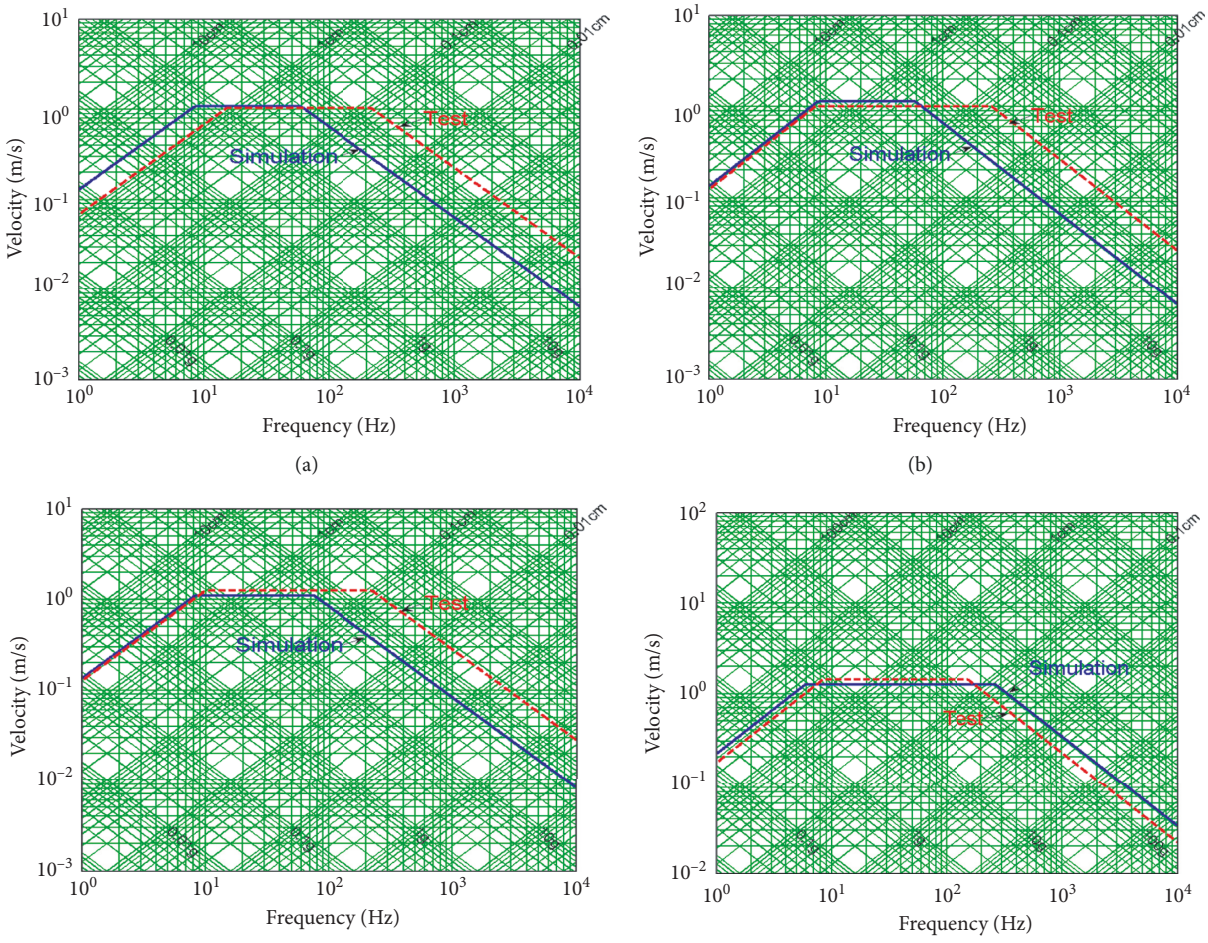

Figure 16: Continued.

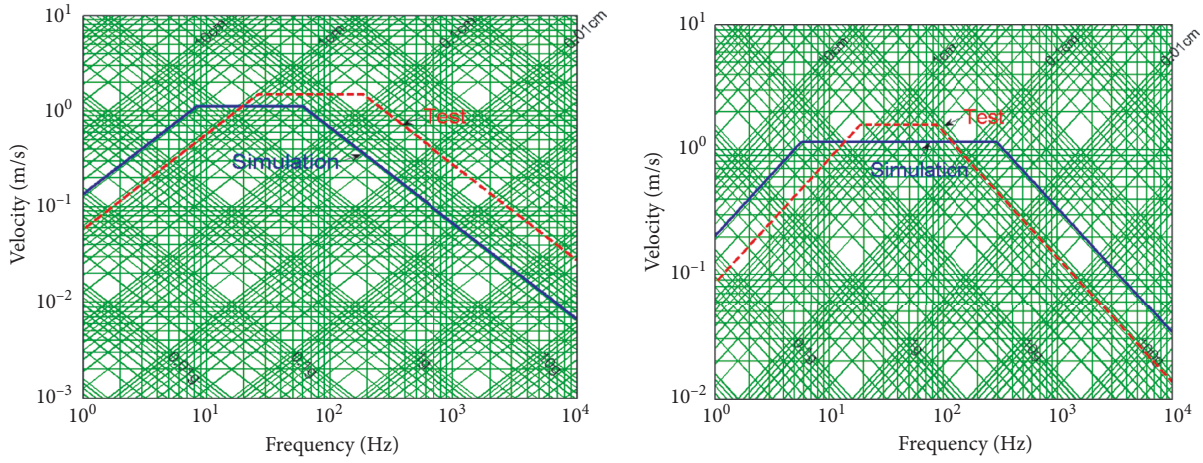

Figure 16: Comparison of the design spectrum of the test points. (a) Horizontal design spectrum at A. (b) Horizontal design spectrum at B. (c) Horizontal design spectrum at C. (d) Vertical design spectrum at C. (e) Horizontal design spectrum at D. (f) Vertical design spectrum at D.

Table 3: Spectral velocity comparison of the platform.

Test point	Horizontal velocity (m/s)			Vertical velocity (m/s)		
	Simulation	Test	Error (%)	Simulation	Test	Error (%)
A	1.08	1.02	5.88	—	—	—
B	1.13	1.00	13.00	—	—	—
C	1.10	1.25	12.00	1.27	1.43	11.19
D	1.12	1.50	25.33	1.15	1.57	26.75
Average value	1.11	1.19	7.13	1.21	1.50	19.33

Table 4: The starboard condition parameters under the same shock factor.

Condition number	1	2	3	4	5	6	7	8	9	10	11	12	13	14	15	16	17	18
The explosion distance of horizontal L (m)	15.5	16.15	16.5	16.85	17.15	17.45	16.35	15.78	15.54	15.26	15.02	15.22	16	16	16	16	16	16
Distance to water surface H (m)	6.5	6.5	6.5	6.5	6.5	6.5	6	7.5	8	8.5	9	10	4.42	5.95	6.98	7.77	8.45	9.04
The weight of the explosive W (kg)	140	150	155	160	165	170	150	150	150	150	150	150	140	145	150	155	160	165

Table 5: The port condition parameters under the same shock factor.

Condition number	19	20	21	22	23	24	25	26	27	28	29	30	31	32	33	34	35	36
The explosion distance of horizontal L (m)	16.6	17.29	17.62	17.95	18.28	18.59	17.11	17.58	17.69	17.78	17.86	17.95	16	16	16	16	16	16
Distance to water surface H (m)	6.5	6.5	6.5	6.5	6.5	6.5	6	7.5	8	8.5	9	10	16.1	18.09	18.95	19.76	20.51	21.23
The weight of the explosive W (kg)	140	150	155	160	165	170	150	150	150	150	150	150	140	150	155	160	165	170

Table 6: Comparison of the structure's average response on the starboard side.

Condition number	1	2	3	4	5	6	7	8	9	10	11	12	13	14	15	16	17	18
Horizontal spectrum velocity (m/s)	1.00	1.09	1.06	1.08	1.08	1.06	1.06	1.05	1.05	1.09	1.04	1.05	1.00	1.05	1.07	1.02	1.06	1.10
Vertical spectrum velocity (m/s)	1.37	1.41	1.43	1.45	1.43	1.42	1.38	1.43	1.41	1.42	1.49	1.43	1.37	1.43	1.41	1.40	1.42	1.48

Table 7: Comparison of the structure's average response on the port side.

Condition number	19	20	21	22	23	24	25	26	27	28	29	30	31	32	33	34	35	36
Horizontal spectrum velocity (m/s)	0.96	1.01	0.99	1.04	0.91	0.94	0.86	1.09	0.97	1.11	0.91	0.87	0.94	0.87	0.88	0.94	0.99	0.94
Vertical spectrum velocity (m/s)	1.85	1.77	1.84	1.84	1.84	1.80	1.82	1.77	1.74	1.85	1.78	1.87	1.62	1.59	1.60	1.62	1.57	1.65

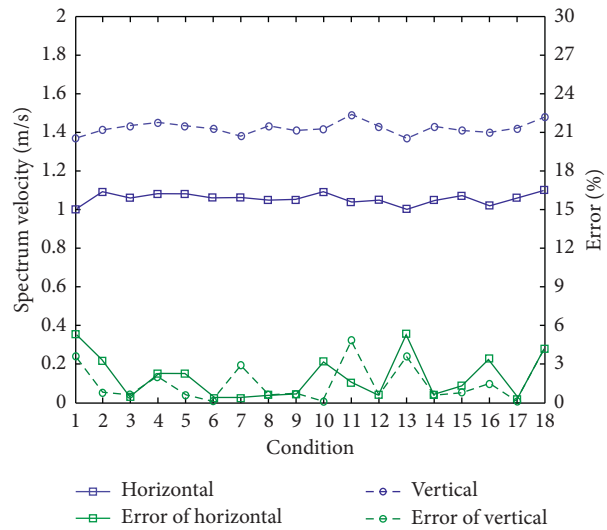

Figure 17: Comparison of the impact response on the starboard side.

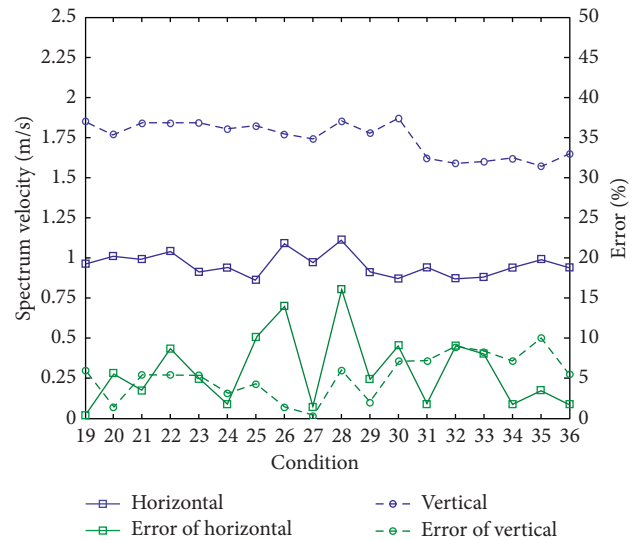

Figure 18: Comparison of the impact response on the port side.

Table 8: Condition setting of impact environment forecast.

Port condition number	1	2	3	4	5	6	7
The explosion distance of horizontal L (m)	5	6	8	12	16	20	24
Distance to water surface H (m)	6.5	6.5	6.5	6.5	6.5	6.5	6.5
The weight of the explosive W (Kg)	150	150	150	150	150	150	150
C_3	12.72	11.69	10.29	8.06	6.51	5.41	4.61
Starboard condition number	8	9	10	11	12	13	14
The explosion distance of horizontal L (m)	5	6	8	12	16	20	24
Distance to water surface H (m)	6.5	6.5	6.5	6.5	6.5	6.5	6.5
The weight of the explosive W (Kg)	150	150	150	150	150	150	150
C_3	13.92	12.94	11.21	8.62	6.88	5.68	4.82

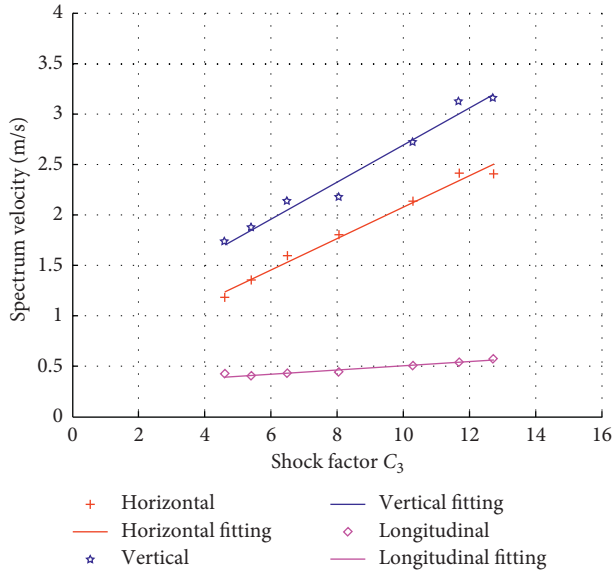

Figure 19: Linear fitting of the impact environment on the starboard side.

horizontal and vertical average response on the starboard side is 5.31% and 4.84%, respectively. Thus, the average shock spectrum response of the platform is essentially consistent on starboard with the same shock factor that effectively describes the shock energy absorbed by platform or the impact strength received by the platform. The maximum error of the horizontal and vertical average response on the port side is 16% and 10%, respectively, which shows that the effect of shock factor is relatively poor on the port side.

4.2. The Prediction of the Impact Environment Based on the Spherical Shock Factor. It has been proved that the shock factor is able to reflect the impact strength of the charge. Therefore, the shock factor is going to be used as the input parameter to study the prediction of the IFSP's impact environment. According to the characteristics of the spherical shock factor, Table 8 presents various conditions set at the port and starboard areas to investigate the impact environment prediction error by shock factor.

The error between the fitting spectrum parameters and actual values is calculated by fitting the data for all conditions; Figures 19 and 20 show the fitting results about spectrum velocity for all conditions, which present a linear relationship between spectrum velocity and shock factor. Table 9 shows all the results about fitting formula and error; it can be seen from the table that except for the longitudinal spectrum velocity and displacement, the shock factor can predict the impact environment well in starboard and port conditions, and the accuracy is within 10%.

To date, no distinct relation or conclusion has been given about the existence of shock factor theory and the structure's response, while the shock factor proposed in this article effectively converts the nonlinear relation into a linear relationship between the input parameters, such as the mass of charge, the explosive distance, and the structural response, so the shock factor presented in this paper has a great significance to the research of the structure's input-output subject to underwater explosion, which can be used to predict the impact environment on IFSP, and the more conditions there are, the higher the prediction accuracy is.

5. Conclusion

(1) In order to study the impact environment characteristics of IFSP subject to underwater explosion, a

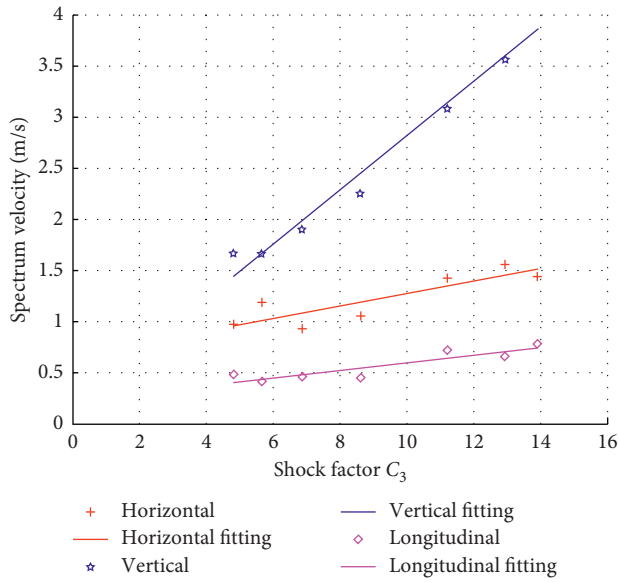

Figure 20: Linear fitting of the impact environment on the port side.

Table 9: Fitting formula and error of spectral parameters.

Spectrum parameter		Port		Starboard	
		Fitting	Error (%)	Fitting	Error (%)
Longitudinal	Displacement (cm)	$0.075C_3 + 1.5$	14.53	$0.029C_3 + 1.8$	14.02
	Velocity (m/s)	$0.038C_3 + 0.22$	10.06	$0.02C_3 + 0.3$	2.46
	Acceleration (g)	$3.1C_3 + 20$	1.58	$3.9C_3 + 7.3$	1.88
Horizontal	Displacement (cm)	$0.23C_3 + 0.2$	3.51	$0.48C_3 - 0.82$	9.89
	Velocity (m/s)	$0.06C_3 + 0.67$	8.81	$0.15C_3 + 0.53$	2.65
	Acceleration (g)	$7.4C_3 + 45$	3.86	$6.5C_3 + 24$	2.73
Vertical	Displacement (cm)	$0.66C_3 - 0.43$	3.51	$0.59C_3 - 0.22$	3.27
	Velocity (m/s)	$0.27C_3 + 0.16$	5.04	$0.18C_3 + 0.87$	2.71
	Acceleration (g)	$17C_3 + 90$	1.97	$11C_3 + 140$	1.61

spherical shock factor about IFSP is defined from the point of energy, and its calculation method is given by the structural characteristics of the platform.

(2) Based on a large number of numerical experiments, the results show that the average response of the platform is essentially consistent with the same shock factor; therefore, the spherical shock factor, as a similarity parameter, can effectively describe the impact environment, that is, the shock energy absorbed by the platform or the impact strength received by the platform.

(3) After changing the charge parameters of various conditions, the results prove that the shock factor proposed in this thesis effectively builds a linear relationship between the input parameters and structural response, and the spectrum parameters are predicted effectively by the shock factor with an error of 10%.

Data Availability

The data used to support the findings of this study are included within the article.

Conflicts of Interest

The authors declare that they have no conflicts of interest.

Acknowledgments

This study was funded by the Special Fund of the Ministry of Industry and Information Technology, China (no. 2018287).

References

[1] BV043/85, *Shock Resistance Specification for Bundeswehr Ships*, German Federal Office for Military Technology and Procurement, 1985.

[2] MIL-S-901D, *Shock Tests, HI (High Impact) Shipboard Machinery Equipment and Systems, Requirements for*, United States Department of Defense, Arlington, VA, USA, 1989.

[3] A.-M. Zhang, S.-F. Ren, Q. Li, and J. Li, "3D numerical simulation on fluid-structure interaction of structure subjected to underwater explosion with cavitation," *Applied Mathematics and Mechanics*, vol. 33, no. 9, pp. 1191–1206, 2012.

[4] H. Cheng, A. M. Zhang, and F. R. Ming, "Study on coupled dynamics of ship and flooding water based on experimental

and SPH methods," *Physics of Fluids*, vol. 29, no. 10, article 107101, 2017.

[5] C.-C. Liang and Y.-S. Tai, "Shock responses of a surface ship subjected to noncontact underwater explosions," *Ocean Engineering*, vol. 33, no. 5-6, pp. 748–772, 2006.

[6] X.-L. Yao, J. Guo, L.-H. Feng, and A.-M. Zhang, "Comparability research on impulsive response of double stiffened cylindrical shells subjected to underwater explosion," *International Journal of Impact Engineering*, vol. 36, no. 5, pp. 754–762, 2009.

[7] W. Zhang and W. Jiang, "An improved shock factor to evaluate the shock environment of small-sized structures subjected to underwater explosion," *Shock and Vibration*, vol. 2015, Article ID 451583, 11 pages, 2015.

[8] J. Guo, X.-B. Ji, Y.-Y. Wen, and X.-W. Cui, "A new shock factor of SWATH catamaran subjected to underwater explosion," *Ocean Engineering*, vol. 130, pp. 620–628, 2017.

[9] J. Greenhorn, "The assessment of surface ship vulnerability to underwater attack," *Royal Institution of Naval Architects Transactions*, vol. 131, 1989.

[10] A. H. Keil, "The response of ships to underwater explosions," in *Proceedings of Annual Meeting of The SNA3E*, vol. 69, pp. 366–410, New York, NY, USA, 1961.

[11] H. A. Gaberson, "Pseudo velocity shock spectrum rules for analysis of mechanical shock," in *Proceedings of IMAC XXV*, Orlando, FL, 2007.

[12] J. N. Martin, A. J. Sinclair, and W. A. Foster, "On the shock-response-spectrum recursive algorithm of Kelly and Richman," *Shock and Vibration*, vol. 19, no. 1, pp. 19–24, 2012.

[13] C. F. Hung, P. Y. Hsu, and J. J. Hwang-Fuu, "Elastic shock response of an air-backed plate to underwater explosion," *International Journal of Impact Engineering*, vol. 31, no. 2, pp. 151–168, 2005.

[14] S. She, "Application of solid angle concept in electromagnetics," *Physics and Engineering*, vol. 14, no. 2, pp. 5–19, 2004, in Chinese.

[15] H. Li, F. Pang, X. Wang, Y. Du, and H. Chen, "Free vibration analysis of uniform and stepped combined paraboloidal, cylindrical and spherical shells with arbitrary boundary conditions," *International Journal of Mechanical Sciences*, vol. 145, pp. 64–82, 2018.

[16] Q. K. Jin and X. B. Ni, "Numerical analysis of dynamic response of ship models subjected to underwater explosion," *International Journal of Nonlinear Sciences and Numerical Simulation*, vol. 11, pp. 201–205, 2010.

[17] C.-Y. Hsu, C.-C. Liang, A.-T. Nguyen, and T.-L. Teng, "A numerical study on the underwater explosion bubble pulsation and the collapse process," *Ocean Engineering*, vol. 81, pp. 29–38, 2014.

[18] G. Barras, M. Souli, N. Aquelet, and N. Couty, "Numerical simulation of underwater explosions using an ALE method. The pulsating bubble phenomena," *Ocean Engineering*, vol. 41, pp. 53–66, 2012.

[19] F. Pang, H. Li, X. Wang, X. Miao, and S. Li, "A semi analytical method for the free vibration of doubly-curved shells of revolution," *Computers & Mathematics with Applications*, vol. 75, no. 9, pp. 3249–3268, 2018.

[20] C. F. Hung, B. J. Lin, J. J. Hwang-Fuu, and P. Y. Hsu, "Dynamic response of cylindrical shell structures subjected to underwater explosion," *Ocean Engineering*, vol. 36, no. 8, pp. 564–577, 2009.